2024 International Conference on Industrial Engineering, Applications and Manufacturing (ICIEAM)

Multivariate Analysis of Multiconductor Transmission Line with Combinational Pulses in Time Response

Evgeniya B. Chernikova
dept. of television and control
Tomsk State University of Control Systems and Radioelectronics
Tomsk, Russian Federation
chiernikova96@mail.ru

***Abstract*—The paper presents a quasi-static simulation of symmetric multiconductor transmission lines (MCTL) with asymmetrical terminations: reflection symmetric meander lines and MCTL with a reference conductor in the form of side polygons. These structures can be used to protect equipment against ultra-wideband interference of short duration. In these MCTLs at connection of two conductors at the far end by a bridge in the time response appear combinational pulses with delays not multiple to per-unit-length delays of modes. The study analyzes the influence of varying cross-section parameters on the characteristics of these structures, including the maximum output amplitude (Umax), the per-unit-length delays of each mode, and the delays of combinational pulses. The study reveals that varying the parameters primarily affects the propagation speed of the main modes, potentially resulting in a rearrangement of their positions. Consequently, combinational pulses, whose delays depend on the mode delays, may arrive at different speeds relative to each other in the process of changing the parameters. The superposition of the pulses leads to a sharp increase in the Umax value. It is demonstrated that previous optimization efforts are ineffective when combinational pulses are present, as they occur between pulses of the main modes, leading to reduced time intervals. These results offer valuable insights for leveraging the resource of combinational pulses in optimization endeavors.**

***Keywords*—radioelectronics, electromagnetic compatibility, transmission lines, time response, combinational pulses, asymmetric structures**

I. Introduction

An essential objective in ensuring electromagnetic compatibility of radio electronic systems is safeguarding against interference [1–4]. Ultra-wideband (UWB) interference pulses, with durations spanning the sub- and nanosecond range, pose significant challenges [5, 6]. These pulses can induce adverse effects in electronic systems, such as signal distortion, device malfunction, damage to sensitive components, and in extreme cases, ignition of electronic elements [7–9]. Given the distinct time and energy characteristics of UWB pulses in modern electromagnetic environment, conventional protection methods like LC- and RC -filters, voltage limiters, and gas dischargers may prove insufficiently effective [10, 11].

Devices employing modal filtering technology have been suggested for protecting radio-electronic equipment from UWB pulses [12]. These devices are able to attenuate the amplitude of interfering pulses by decomposing them down into smaller amplitude pulses, leveraging the difference in the per-unit-length delays of modes ($\Delta\tau_i$) propagating in the multiconductor transmission lines (MCTLs) with inhomogeneous dielectric filling [13]. The protective characteristics include the attenuation determined by the maximum amplitude of decomposition pulses at the output of the structures (U_{max}), along with the maximum duration (t_Σ) of the interfering UWB pulse, which depends on the minimum value of time intervals between decomposition pulses. During the study of asymmetric MCTLs with modal decomposition, it has been observed that the time response of such lines exhibits combinatorial pulses with delays that are not multiples of the per-unit-length delays of modes [14]. It has been determined that combinatorial pulses represent a new resource for optimization, thereby enhancing the efficacy of such protective devices [15]. However, before performing the optimization, it is necessary to calculate and evaluate the influence of cross-section parameters on the characteristics of MCTLs with combinatorial pulses in the time response. Thus, the purpose of this study is to perform a multivariate analysis of MCTLs with symmetric cross-sections and asymmetric terminations.

II. Simulation Approaches

The calculation and evaluation of the influence of geometrical parameters on the characteristics of MCTLs with modal decomposition are exemplified using the reflection symmetric meander line (ML) and MCTL with a reference conductor in the form of side polygons. Their cross-sections are shown in Fig. 1, where: w is the width of the signal conductors, s is the distance between the signal conductors, t is the thickness of the conductors, h is the dielectric thickness, $w1$ is the width of the reference conductors, d is the distance between the reference and signal conductors, ε_r is the relative dielectric constant of the substrate.

Both MCTLs are a 4-conductor line, with the two conductors at the far end connected by a bridge in three diagrams (Fig. 2). This ensures the propagation of the 4 main modes (A, B, C, D) as well as the presence of combinational

The research was funded by the Russian Science Foundation, project 22-79-00187, https://rscf.ru/project/22-79-00187/ at TUSUR.

pulses in the time response of the MCTLs. The delays of these pulses are equal to the arithmetic mean of the doubled per-unit-length delays of the modes or alternatively, their sum [16]. Because the combinational pulses are located between the pulses of the main modes, the time interval diminishes by a factor of 2. Consequently, the previous optimization of the initial MCTLs (without bridge) based on the criterion of equalization of time intervals between the decomposition pulses is not effective. Hence, it becomes imperative to ascertain the influence of varying the cross-section parameters on the characteristics of MCTLs, specifically on the values of U_{max}, the per-unit-length delays of each mode (τ_i), and the delays of combinational pulses ($\tau_i+\tau_j$).

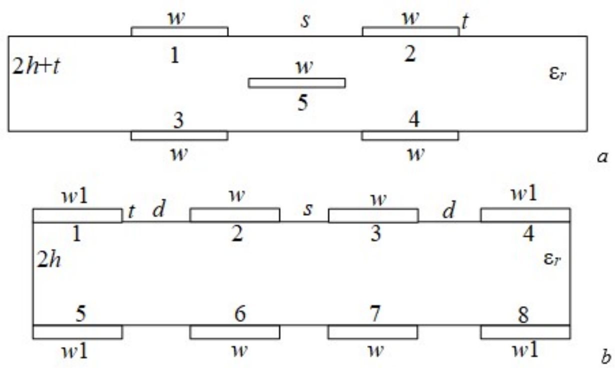

Fig. 1. Cross sections of reflection symmetric ML (*a*) and MCTL with a reference conductor in the form of side polygons (*b*).

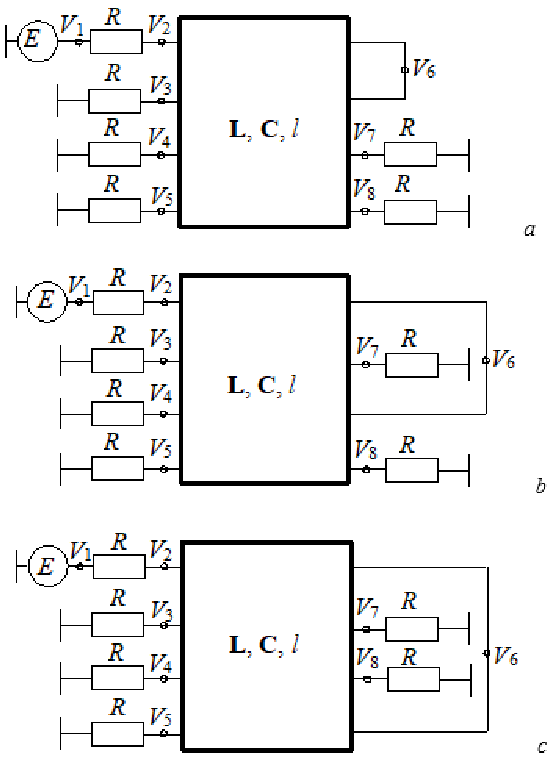

Fig. 2. Electrical connection diagrams of MCTLs with the two conductors at the far end connected by a bridge: 1 (*a*) 2 (*b*) and 3 (*c*).

For this purpose, lossless quasi-static simulation is performed using TALGAT software [17]. The method of moments (MoM) is used to obtain the matrices of per-unit-length coefficients of electrostatic (**C**) and electromagnetic (**L**) inductions [18]. The segmentation parameters are set to 5 segments per conductor end, 50 segments along the conductor width, and 80 segments along the dielectric width [19]. The mathematical model from [20] is used to calculate the time response. An electromotive force source with an amplitude of 5 V and durations of rise, fall and flat top each set to 50 ps is selected as the test stimulus. The length of the MCTLs is 1 m, and the resistors values on the diagram is set to R=50 Ω.

III. Simulation Results

To evaluate the influence of parameters on MCTL characteristics, simulation was performed across the parameter ranges: *s* and *w* from 0.1 to 3 mm with a step of 0.2, *w*1 from 1 to 3 mm with a step of 0.2, *d* from 1.5 to 10 mm with a step of 0.5, *h* from 0.1 to 2 mm with a step of 0.5, *t* at 18, 35, 70, and 105 µm. The plots of the dependencies of U_{max} values on parameters *s*, *w*, *h*, and *t* for each MCTLs are presented in Table I. Notably, the per-unit-length parameter values solely depend on MCTL parameters and remain unaffected by diagram variations. Thus, the per-unit-length delays for all diagrams will be the same are given in Table II. The dependence plots of combinational pulse delay values are given in Table III. The parameters *w*1 and *d* exhibit minimal impact on both main and combinational pulse delays, thus their dependency graphs are omitted from this discussion.

A. MCTL with a Reference Conductor in the Form of Side Polygons

Analysis of the characteristics at the output of diagram 1 reveals the following observations. Increasing parameter *s* results in convergence of the linear delays of modes *A* and *B*, *C* and *D*, respectively, leading to a pair-wise superposition of two pulses. The variation in parameter *s* affects the combinational pulses. Specifically, up to *s*=0.5 mm, the combinational pulse with delay $\tau_b+\tau_c$ precedes the pulse with delay $\tau_d+\tau_a$; at *s*=0.5 mm, their superposition occurs, after which they interchange positions. With an increase in parameter *w*, there is a noticeable augmentation in the difference in per-unit-length delays of modes *B* and *C*, while the discrepancies in per-unit-length delays of modes *A* and *B*, *C* and *D* remain constant. Additionally, the delay values of combinational pulses increase with increasing parameter *w*. Increasing parameter *h* leads to equalization of all per-unit-length delays, resulting in the superposition of all pulses. At lower values of *h*, the combinational pulse with delay $\tau_d+\tau_a$ precedes the combinational pulse with delay $\tau_b+\tau_c$; at *h*=0.25 mm, both combinational pulses have equivalent delays, after which they swap positions. Parameter *t* has minimal influence on per-unit-length delays, but its increment induces changes in combinational pulse delays, such that at *t*=105 µm, they interchange positions. Increasing parameter *s* up to 0.5 mm results in an initial rise followed by a subsequent decrease in the maximum amplitude, which stabilizes to a constant U_{max} value after *s*=1 mm. This behavior arises from the separation of pulses that were previously superimposed on each other as *s* increases. Increasing parameter *w* leads to a decrease in the value of U_{max}. However, at *h*=1 mm, the value of U_{max} increases due to the superposition of pulses.

Analysis of the characteristics at the output of diagram 2 reveals the following insights. Changing parameter *s* does not influence the combinational pulses. The delays of combinational pulses increase with increasing parameter *w*. Parameter *t* have minimal effect on combinational pulse delays. Increasing parameter *h* results in equalization of all combinational pulse delays. Consequently, at *h*=2 mm, there will be overlapping of combinational pulses. Increasing parameters *s* and *w* leads to an increase in the value of U_{max}, but parameter *t* has negligible effects on U_{max}. Increasing parameter *h* leads to an increase in U_{max} due to the superposition of pulses.

TABLE I. DEPENDENCE OF U_{MAX} VALUE AT THE OUTPUT OF THE DIAGRAMS ON THE CROSS-SECTION PARAMETERS OF THE MCTLS

Structures	Diagrams	Parameters			
		s	**w**	**h**	**t**
Reflection symmetric ML	1	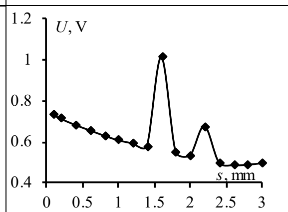	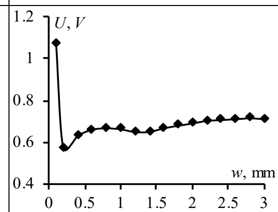	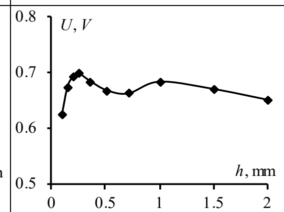	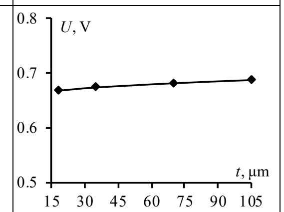
	2	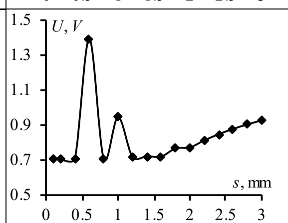	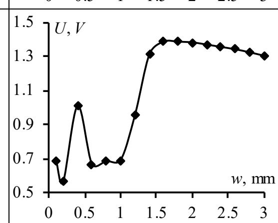	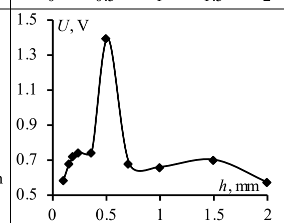	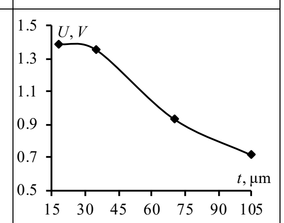
	3	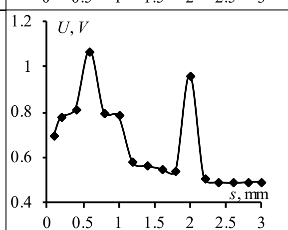	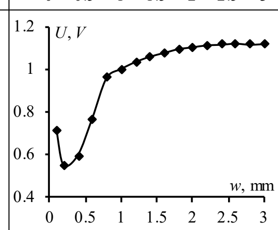	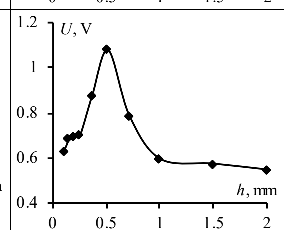	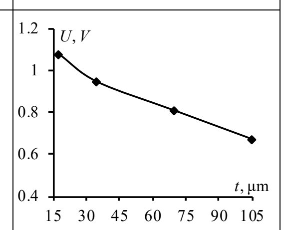
MCTL with a reference conductor in the form of side polygons	1	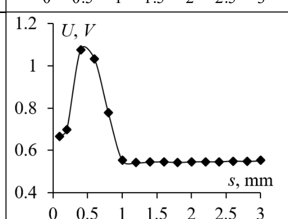	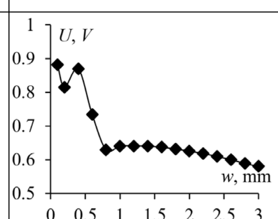	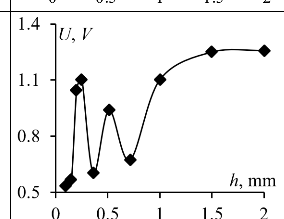	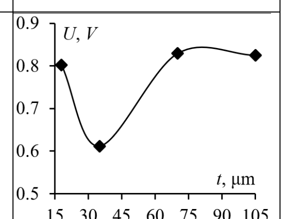
	2	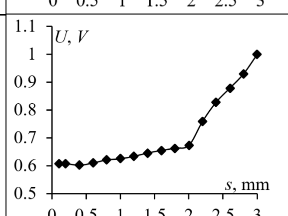	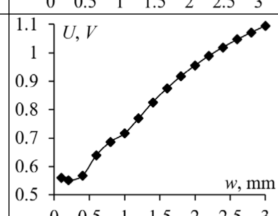	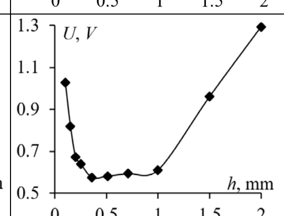	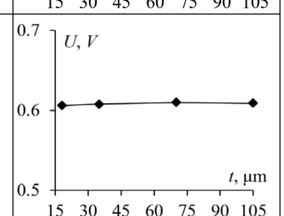
	3	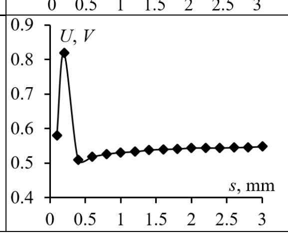	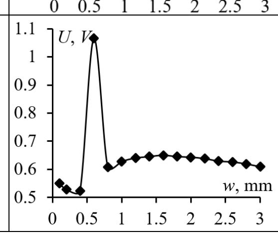	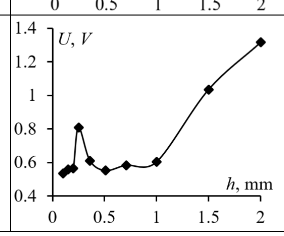	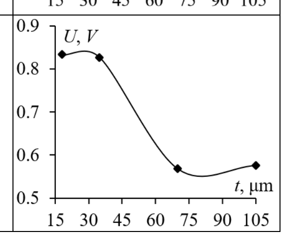

TABLE II. DEPENDENCES OF THE VALUES OF PER-UNIT-LENGTH DELAYS OF MODES (τ_i) AT THE OUTPUT OF THE DIAGRAMS

Structures	Diagrams	Parameters: *s*	*w*	*h*	*t*
Reflection symmetric ML	1, 2 and 3	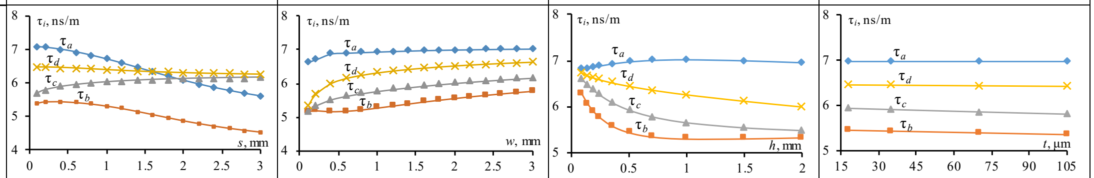			
MCTL with a reference conductor in the form of side polygons	1, 2 and 3	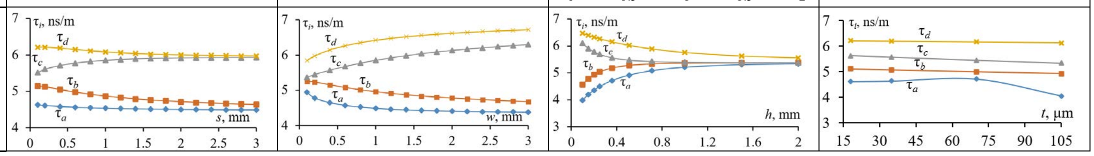			

TABLE III. DEPENDENCES OF THE VALUES OF COMBINATION PULSE DELAYS($\tau_i+\tau_j$) AT THE OUTPUT OF THE DIAGRAMS

Structures	Diagrams	Parameters: *s*	*w*	*h*	*t*
Reflection symmetric ML	1	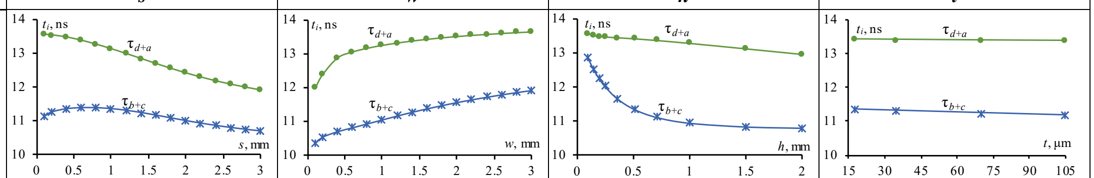			
	2	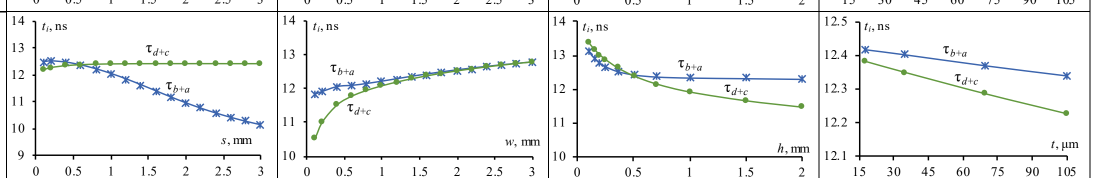			
	3	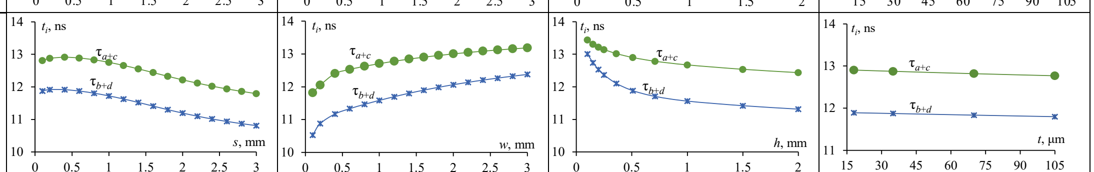			
MCTL with a reference conductor in the form of side polygons	1	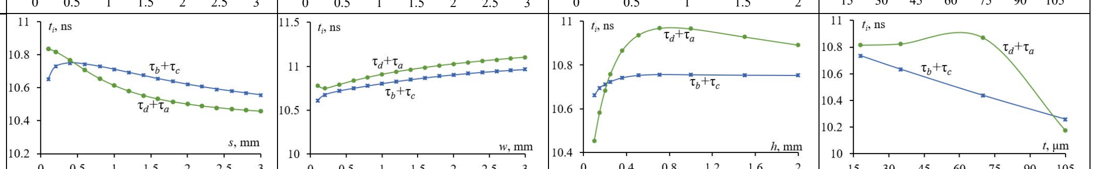			
	2	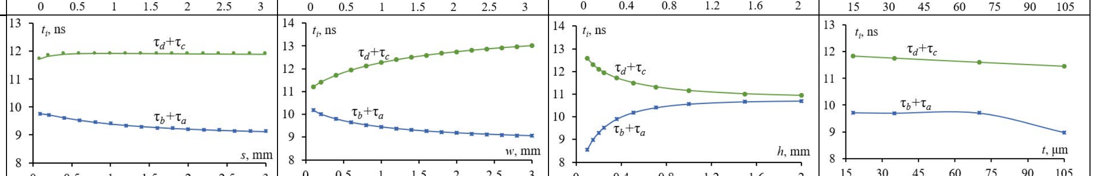			
	3	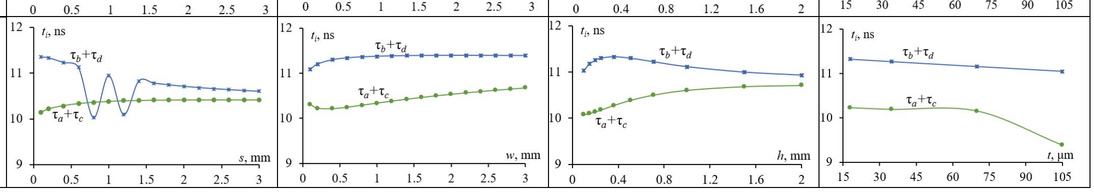			

The analysis of characteristics at the output of diagram 3 reveals the following observations. Changing parameter *s* affects the combinational pulse with delay $\tau_b+\tau_d$. Specifically, at *s*=0.8 mm and 1.2 mm, this pulse precedes the pulse with delay $\tau_a+\tau_c$, while at other *s* values, the combinational pulse $\tau_a+\tau_c$ comes first. Parameters *w*, *h*, and *t* have minimal effect on the delays of combinational pulses. Increasing parameters *s* and *w* minimally affect U_{max}, except for instances where a sharp increase in amplitude occurs (at *s*=0.2 mm and *w*=0.6 mm). Increasing *h* leads to an increase in U_{max}, while increasing parameter *t* results in a decrease.

B. Reflection symmetric ML

Analysis of the characteristics at the output of diagram 1 reveals the following insights. Increasing parameter *s* influences the per-unit-length delays of modes *A*, *B*, *C*, and *D*. Variation in *s* causes modes *A*, *C*, and *D* to interchange positions among themselves, while mode *B* remains unchanged (being the fastest). Mode *A*, initially the slowest at small values of *s*, transitions to being second to last as *s* approaches 3 mm. Conversely, modes C and D, initially the second and third slowest at small *s*, become the third and fourth slowest as the conductors move farther apart. However, the delays of these modes are minimally affected by parameter *s*, with the change in delay order primarily due to a significant alteration in delay of mode *A*. Increasing parameters *w* and *h* results in an augmentation of the differences in linear delays of the main modes. At *h*=0.1 mm and *w*=0.1 mm, modes *A*, *C*, and *D* exhibit nearly identical values. Parameter *t* does not influence the per-unit-length delays. The variation of cross-section parameters does not alter the pattern of change in combinational pulse delays: they decrease smoothly with increasing *s* and *h*, increase smoothly with increasing *w*, and remain unaffected by changes in *t*. Increasing *s* has a negligible effect on U_{max}, except for two instances where a sharp increase in maximum amplitude is observed (at *s*=1.6 mm and 2.2 mm). At *w*=0.1 mm, a high U_{max} is initially observed, followed by a sharp decrease and subsequent stabilization. Increasing *h* and *t* does not affect U_{max}.

Analysis of the characteristics at the output of diagram 2 reveals the following insights. Changing parameter *s* affects the delays of combinational pulses. At *s*=0.6 mm, the combinational pulses interchange positions. Altering *h* also results in a change in the order of arrival of combinational pulses (at *h*=0.5 mm). Increasing parameter *w* reduces the delay values of combinational pulses to a single value, facilitating their superposition. Increasing *t* leads to a decrease in the delays of combinational pulses. Increasing *s* has a minor effect on U_{max}, except for two instances where there is a sharp increase in maximum amplitude (at *s*=1.6 mm and 1 mm). At *w*=0.4 mm, there is a sharp increase in U_{max}, followed by a continuous increase, stabilizing after *w*=1.4 mm. Increasing *h* has minimal influence on U_{max}, except for a moment where there is a sharp increase (at *h*=0.5 mm). Increasing *t* leads to a decrease in U_{max}.

Analysis of the characteristics at the output of diagram 3 reveals the following insights. Increasing *s*, *w*, and *h* results in a gradual change in the delays of combinational pulses. Specifically, their delays decrease with increasing *s* and *h*, while they increase with increasing *w*. However, increasing parameter *t* does not affect the delays. Increasing *s* generally leads to a decrease in the value of U_{max}, except at two specific points where there is a sharp increase (at *s*=0.6 mm and 2 mm). Increasing *h* leads to an increase in the value of U_{max} up to *h*=0.5 mm, after which it gradually decreases. However, increasing parameter *t* results in a decrease in the value of U_{max}.

IV. Discussion of Results

These results are preliminary findings for the subsequent optimization of MCTL utilizing the resource of combinational pulses. Before performing the optimization, it should be noted that the previous assumption regarding combinational pulses, stating they consist of combinations of delays from the fastest and slowest modes, irrespective of their propagation mode, needs reassessment [15]. Through this study, it has been revealed that combinational pulses are comprised specifically of combinations of propagation modes *A*, *B*, *C*, and *D*. Additionally, their velocities can vary depending on parameter variations. Hence, the earlier assumption holds true only for a particular structure with specific cross-section parameters. Depending on changes in coupling strength (e.g., strengthening or weakening of broad-side or edge coupling), pulses corresponding to various modes may arrive with different delays. Moreover, a single combinational pulse, under certain cross-section parameters, can consist of delays from modes that arrived first and third, while under different parameters, it may involve delays from modes that arrived first and second. Nevertheless, the mode of propagation remains consistent; thus, in both cases, the combination includes mode *B* and mode *C*. Consequently, the delays of combinational pulses are contingent on the delays of modes within a specific propagation mode and are unaffected by the order of pulse arrival. This fact is important for subsequent optimization by the criterion of time interval equalization.

V. Conclusion

Thus, the results of estimation of amplitudes and per-unit-length delays of decomposition pulses, including combinational ones, are presented. The influence of changing the cross-section parameters on the characteristics of three diagrams of MCTL with side polygons and reflection symmetric ML is shown. It is revealed that parameter changes primarily influence the propagation speed of the main modes, potentially resulting in their interchange. Consequently, combinational pulses, whose delays are contingent on mode delays, may exhibit varying arrival times relative to each other during parameter alterations. The U_{max} value at the output of the MCTL mainly hinges on pulse arrival times. Their superposition leads to a significant increase in U_{max}. These findings are instrumental for further optimization of MCTLs utilizing the resource of combinational pulses. Based on the results of parameter influence evaluation on structure characteristics, appropriate ranges for he ranges of parameter changes can be selected. In addition, the peculiarities of determining combinational pulse delays are delineated, which is pivotal for subsequent optimization based on the criterion of time interval equalization, where pulse arrival time holds principal importance.

References

[1] M. Kučera and M. Šebök, “Electromagnetic compatibility analysing of electrical equipment,” 2016 Diagnostic of Electrical Machines and Insulating Systems in Electrical Engineering (DEMISEE), Papradno, Slovakia, 2016, pp. 104–109.

[2] L. Duipmans, D. Milosevic, A. van der Wel and P. Baltus, “Distortion contribution analysis for identifying EM immunity failures,” in IEEE

Transactions on Circuits and Systems I: Regular Papers, vol. 67, no. 8, pp. 2767–2779, Aug. 2020.

[3] E. P. Li, et al., "Progress review of electromagnetic compatibility analysis technologies for packages, printed circuit boards, and novel interconnects," in IEEE Transactions on Electromagnetic Compatibility, vol. 52, no. 2, pp. 248–265, May 2010.

[4] W. A. Radasky and M. W. Wik, "Overview of the threat of intentional electromagnetic interference (IEMI)," 2003 IEEE International Symposium on Electromagnetic Compatibility, 2003. EMC '03., 2003, pp. 1024–1027.

[5] N. Mora, F. Vega, G. Lugrin, F. Rachidi and M. Rubinstein, "Study and classification of potential IEMI sources," System and assessment notes, Note 41, p. 92, 8 July 2014.

[6] T. Weber, R. Krzikalla and J. L. ter Haseborg, "Linear and nonlinear filters suppressing UWB pulses," in IEEE Transactions on Electromagnetic Compatibility, vol. 46, no. 3, pp. 423–430, Aug. 2004.

[7] H. Nishiyama, T. Okamoto, Y. Kim, D. Fujimoto and Y. -i. Hayashi, "Fundamental study on influence of intentional electromagnetic interference on IC communication," 2019 12th International Workshop on the Electromagnetic Compatibility of Integrated Circuits (EMC Compo), 2019, pp. 201–203.

[8] Z. M. Gizatullin and R. M. Gizatullin, "Investigation of the immunity of computer equipment to the power-line electromagnetic interference," Journal of Communications Technology and Electronics, no. 5, pp. 546–550, 2016.

[9] C. Mojert, "UWB and EMP susceptiblity of microprocessors and networks," Proc. of the 14th International Zurich symposium on electromagnetic compatibility, Zurich, Switzerland, 2001, pp. 47–52.

[10] M. Camp, H. Garbe and D. Nitsch, "UWB and EMP susceptibility of modern electronics," 2001 IEEE EMC International Symposium. Symposium Record. International Symposium on Electromagnetic Compatibility (Cat. No.01CH37161), vol.2, Montreal, QC, Canada, 2001, pp. 1015–1020.

[11] I. F. Kovačević, T. Friedli, A. M. Müsing and J. W. Kolar, "3-D electromagnetic modeling of parasitics and mutual coupling in EMI Filters," in IEEE Transactions on Power Electronics, vol. 29, no. 1, pp. 135–149, Jan. 2014.

[12] A. T. Gazizov, A. M. Zabolotsky, T. R. Gazizov, "UWB pulse decomposition in simple printed structures," in IEEE Transactions on Electromagnetic Compatibility, vol. 58, no. 4, pp. 1136–1142, Aug. 2016.

[13] T. R. Gazizov, A. M. Zabolotsky, "New approach to EMC protection," 2007 18th International Zurich Symposium on Electromagnetic Compatibility, Munich, Germany, 2007, pp. 273–276.

[14] A. T. Gazizov, A. M. Zabolotsky and T. T. Gazizov, "Time-domain response of asymmetrical modal filter without resistors to ultrashort pulse excitation," 2016 17th International Conference of Young Specialists on Micro/Nanotechnologies and Electron Devices (EDM), Erlagol, Russia, 2016, pp. 85–88.

[15] A. O. Belousov, E. B. Chernikova, et al., "From symmetry to asymmetry: the use of additional pulses to improve protection against ultrashort pulses based on modal filtration," Symmetry, vol. 12, no. 7, pp. 1–38, 2020.

[16] E. B. Chernikova and Y. S. Zhechev, "Time response analysis for reflection symmetric meander lines using quasistatic and electrodynamic approaches," 2022 International Conference on Actual Problems of Electron Devices Engineering (APEDE), Saratov, Russian Federation, 2022, pp. 101–104.

[17] S. P. Kuksenko, "Preliminary results of TUSUR University project for design of spacecraft power distribution network: EMC simulation," IOP Conf. Series: Materials Science and Engineering, vol. 560, no. 012110, pp. 1–7, 2019.

[18] R. F. Harrington, "Matrix methods for field problems," in Proceedings of the IEEE, vol. 55, no. 2, pp. 136–149, Feb. 1967.

[19] A. E. Maksimov, S. P. Kuksenko, "On the features of calculating per-unit-length parameters and characteristics of multiconductor transmission lines," Journal of Communications Technology and Electronics, vol. 68, no. 12, pp. 1412–1429, March 2023.

[20] R. Achar and M. S. Nakhla, "Simulation of high-speed interconnects," in Proceedings of the IEEE, vol. 89, no. 5, pp. 693–728, May 2001.